# Emergence of Spin-Half Fermion Vortices and The Vortex Metal

Netanel Lindner[1], Assa Auerbach[1] and Daniel P. Arovas[2]
*1) Physics Department, Technion, 32000 Haifa, Israel*
*2) Department of Physics, University of California at San Diego, La Jolla, CA 92093, USA*

We present two theoretical findings concerning quantum properties of vortices of two dimensional lattice bosons, at half filling. First, we provide a rigorous proof of doublet degeneracies for any odd vorticity on finite tori. The result is made physical by connecting the doublets to a *local* spin half (v-spin) carried by each vortex. The v-spins have experimental consequences in the normal superfluid (vortex lattice) phase. Second, building on the first result, we discover numerically that two vortex wavefunctions obey Fermi-Dirac statistics: a demonstration of 'statistical transmutation' in a generic bosonic model. The multi-vortex system undergoes quantum melting at low vortex density ($\sim 10^{-3}$/site). The resulting Vortex Metal features a 'Fermi temperature' and unusual transport behavior. Experiments in cold atoms on optical lattices, low capacitance Josephspon arrays and low superfluid density superconductor films in a magnetic field, could test our predictions.

Condensed matter systems are made out of fermions and bosons. Their interactions may lead to emergent low energy quasiparticles with different statistics than their constituents. Famous examples are Cooper pairs [1] in superconductors, and statistical transmutations of electrons into 'anyons' in Quantum Hall phases [2]. Point vortices appear in two dimensional superfluids when subjected to a rotation [3, 4, 5] (or a magnetic field if the bosons carry charge). A great deal of thermodynamics and transport properties could be understood by treating them as classical particles [6, 7, 8]. Quantum effects are experimentally relevant at low temperatures, when vortices can tunnel between pinning sites [9, 10, 11]. As quantum particles, the obvious questions are: *do vortices carry internal quantum numbers*? and *are they bosons or fermions*? We address these questions in this paper.

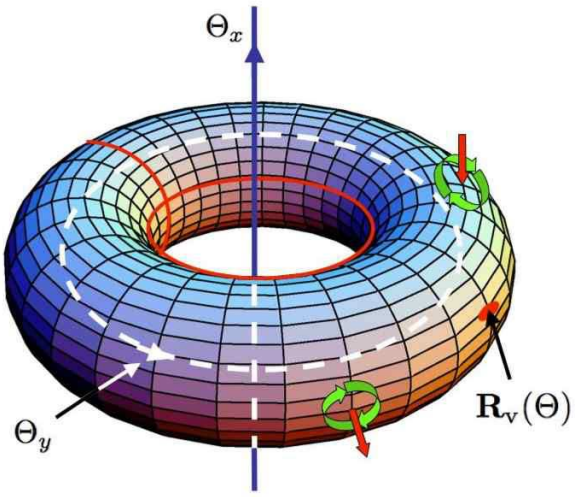


FIG. 1: The geometry used to determine vortex spin and statistics. The torus is penetrated by a uniform magnetic field, and threaded by two Aharonov Bohm fluxes $\mathbf{\Theta} = (\Theta^x, \Theta^y)$. The red circles denote zero flux orbits, which intersect at a gauge invariant *null point* $\mathbf{R}_0$. The antipodal position $\mathbf{R}_v(\mathbf{\Theta})$, is where the vortex center of mass is localized. The symmetry operators $\mathbf{\Pi}$ are defined about $\mathbf{R}_v$. Two static vortices are illustrated by green circulating currents, and red arrows depict their v-spins.

The vortex lattice (superfluid) phase may melt by quantum fluctuations. The resulting quantum vortex liquid crucially depends on vortex statistics.

To put it simply: vortices which obey Bose statistics should 'Bose-condense' at low temperatures and create a charge-gapped Mott insulator [12]. The other, perhaps more 'exotic' possibility, is for vortices to be *fermions* and condense into a Fermi liquid (made of bosons!). Then the

viscosity (or resistivity for charged bosons) may level off at low temperatures and a Vortex Metal (VM) would emerge. Recently, metallic phases of bosons and vortices have been proposed [13, 14] to explain low temperature resistivity in superconductor films [15, 16, 17].

The semiclassical Berry-phase method of determining quasiparticle statistics [18], is inconclusive for superfluid vortices [19]. The problem arises due to the long ranged nature of their density depletion.

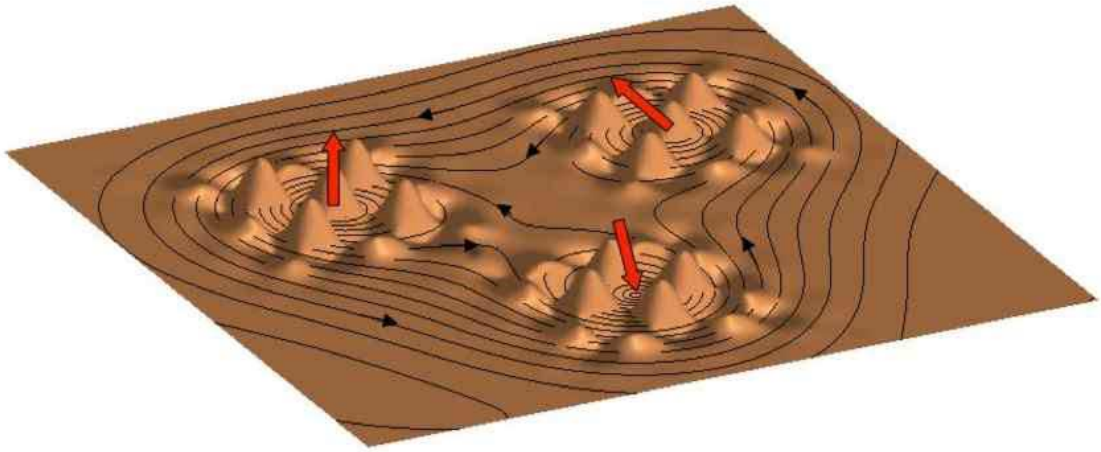

FIG. 2: Illustration of three static vortices with their v-spins. Arrows describe the v-spin directions, their $z$-component is the local charge density wave near the vortex core, illustrated as ripples in the surface. Current density is depicted by black field lines.

Here we report on progress achieved by a different approach. Sidestepping the semiclassical difficulties, we directly study the quantum eigenstates of lattice bosons at half filling on a torus depicted in Fig. 1. Using this geometry we can control both the number of vortices and their center of mass by tuning the gauge field. We further localize individual vortices by weakening appropriate bonds. Now that we've got their attention, we can study their quantum dynamics and symmetries.

The vortex spin, statistics and mass are extracted from degeneracies, symmetries and fits of the exact spectrum to simple Hamiltonians of spin half fermions. We prove that vortices carry local spin half (v-spin), as illustrated in Fig. 2. Numerical evidence indicates that two vortices exhibit *Fermi statistics* under permutation. We derive the coupling constants for the multi-vortex Spin Half Fermion Plasma (SHFP) model. It describes a gas of logarithmically interacting spin half fermions, with a neutralizing background charge and spin orbit coupling.

The SHFP connects the small lattice results to experimental realizations in: rotating cold atoms on partially filled optical lattices [3, 4, 5], gated low capacitance Josephson Junction arrays[20], and indirectly to physics of disordered low superfluid density superconductor films [15, 16, 17].

In the Vortex Lattice (VL) superfluid phase, signatures of v-spin correlations should be observable at low temperatures. The VL is predicted to undergo quantum melting at a density lower than $10^{-3}$ vortices per site. The most striking manifestation of vortex Fermi statistics would be a confirmation of the VM phase, with its Fermi temperature and unusual transport.

In the discussion, we relate our theory to previous work, and mention future extensions. Technical details are provided in the supplemental material [21].

**The Model.** The quantum mobility of a vortex in a weakly disordered superfluid is very low: it decays as a gaussian of the ratio between tunneling distance to boson separation [9, 11]. A large vortex mobility is expected for strongly interacting bosons in a periodic potential.

We consider therefore the limit of *hard core* bosons at a density of half a boson per site. A generic model with hopping parameter $t$, nearest neighbor repulsion $V < t$,

and lattice constant $a$, is

$$\mathcal{H} = \sum_{\langle \mathbf{r},\mathbf{r}'\rangle} -\frac{t}{2}\left(e^{i\int_{\mathbf{r}}^{\mathbf{r}'} d\mathbf{l}\cdot\mathbf{A}}\, a^\dagger_{\mathbf{r}} a_{\mathbf{r}'} + \text{h.c.}\right) + V n_{\mathbf{r}} n_{\mathbf{r}'}. \quad (1)$$

$a^\dagger_{\mathbf{r}}$ creates a hard core boson at site $\mathbf{r}$, with occupations restricted to $n_{\mathbf{r}} = 0, 1$ [22]. The sum runs over nearest neighbors bonds of the square lattice with an even number of sites. The lattice is embedded periodically on a torus of dimensions $\mathbf{L} = (L_x, L_y)$ as shown in Fig.1. The gauge field $\mathbf{A}$ describes a uniform magnetic field with a total of $N_\phi$ flux quanta, and a pair of Aharonov Bohm (AB) fluxes $\mathbf{\Theta} = (\Theta^x, \Theta^y)$, which thread the two holes of the torus. Two gauge invariant Wilson loop functions are given by

$$\Phi^y(x) = \oint dy A^y(x,y), \quad \Phi^x(y) = \oint dx A^x(x,y). \quad (2)$$

The intersection of the lines $\Phi^x = 0, \Phi^y = 0$, depicted as red lines in Fig. 1, is a *null point* $\mathbf{R}_0$ which is a gauge invariant symmetry point on the torus. For $N_\phi > 1$ there are $N_\phi^2$ such points. The null point can be moved anywhere on the torus *continuosly* (i.e. even between lattice sites), by changing the AB fluxes,

$$\mathbf{R}_0(\mathbf{\Theta}) = \frac{1}{2\pi N_\phi}\mathbf{L}\times\mathbf{\Theta} + \mathbf{R}_0(0,0) \text{ mod } \mathbf{L}. \quad (3)$$

The antipodal point to the null point is denoted by $\mathbf{R}_{\rm v}(\mathbf{\Theta}) = \frac{1}{2}\mathbf{L} + \mathbf{R}_0$. Variationally, the vortex center of mass is confined by a potential which has its minimum at $\mathbf{R}_{\rm v}$ [21].

**Degeneracies**. We follow the standard route to proving quantum degeneracies [23, 24] by constructing a non abelian algebra of symmetry operators.

For $N_\phi > 0$, $\mathcal{H}$ does *not* possess the full lattice translational symmetry. In particular, for $N_\phi = 1$ there are no translational symmetries. Nevertheless, we can exploit point group symmetries about $\mathbf{R}_{\rm v}$, which we tune (by $\mathbf{\Theta}$) to be on any lattice site. Two special operators are constructed:

$$\Pi^\alpha[\mathbf{R}_{\rm v}] = U^\alpha C P^\alpha[\mathbf{R}_{\rm v}], \quad \alpha = x, y, \quad (4)$$

where $P^{x(y)}[\mathbf{R}_{\rm v}]$ is the lattice reflection about $x(y)$ axis passing through $\mathbf{R}_{\rm v}$. The charge conjugation $C$ sends $n_{\mathbf{r}} \to 1 - n_{\mathbf{r}}$. We construct [21] the gauge transformation $U^\alpha[\mathbf{A}, \mathbf{R}_{\rm v}]$ such that

$$\left[\Pi^x[\mathbf{R}_{\rm v}], \mathcal{H}[\mathbf{\Theta}]\right] = \left[\Pi^y[\mathbf{R}_{\rm v}], \mathcal{H}[\mathbf{\Theta}]\right] = 0 \quad (5)$$

A straightforward, though somewhat lengthy algebra [21], arrives at the important relation

$$\Pi^x\Pi^y = (-1)^{N_\phi}\Pi^y\Pi^x \equiv i\Pi^z. \quad (6)$$

The operators $\mathbf{\Pi}^\alpha = (\Pi^x, \Pi^y, \Pi^z)$ are unitary and hermitian, and therefore their eigenvalues are $\pm 1$. For odd $N_\phi$, each common eigenstate of $\mathcal{H}, \Pi^z$, labelled by $|E, \pi^z\rangle$ is orthogonal to its degenerate partner $|E, -\pi^z\rangle$ obtained by acting on it with $\Pi^x$. Therefore, Kramer's degeneracies are proven. The operators $\boldsymbol{\tau} = \frac{1}{2}\mathbf{\Pi}$ define an SU(2) algebra of spin half, $[\tau^\alpha, \tau^\beta] = i\epsilon_{\alpha\beta\gamma}\tau^\gamma$ where $\epsilon$ is the antisymmetric tensor.

For a single vortex $N_\phi = 1$, we define $\boldsymbol{\tau}$ as the v-spin associated with a vortex at $\mathbf{R}_{\rm v}$.

For multiple vortices, the Kramers degeneracies appear for any odd number of vortices, consistent with the behavior of a general interacting system of spin half particles. We can use $\Pi^z$ to rotate the eigenstates by 180° around $\mathbf{R}_{\rm v}$. A separate measure of v-spin density of individual vortices is required.

The v-spin density is defined as the modified topological density

$$\tau^z(\mathbf{r}) \simeq \frac{1}{4\pi}\hat{\mathbf{n}}\cdot D_x\hat{\mathbf{n}}\times D_y\hat{\mathbf{n}}, \quad (7)$$

where $D_\alpha$ are gauge invariant derivatives. $\hat{\mathbf{n}}$ is the vector order parameter, whose $xy$ components are the superfluid order $\hat{\mathbf{n}}^x_{\mathbf{r}} + i\hat{\mathbf{n}}^y = a^\dagger_{\mathbf{r}}$, and $z$ component is the charge density wave $\hat{\mathbf{n}}^z_{\mathbf{r}} = (-1)^{(x+y)/a}(n_{\mathbf{r}} - \frac{1}{2})$, as depicted in Fig. 2.

A classical single vortex field is a *meron* (half a skyrmion) whose topological charge in the continuum limit (and $\mathbf{A} = 0$), is $Q = \int d^2r\ \tau^z(\mathbf{r}) = \pm\frac{1}{2}$.

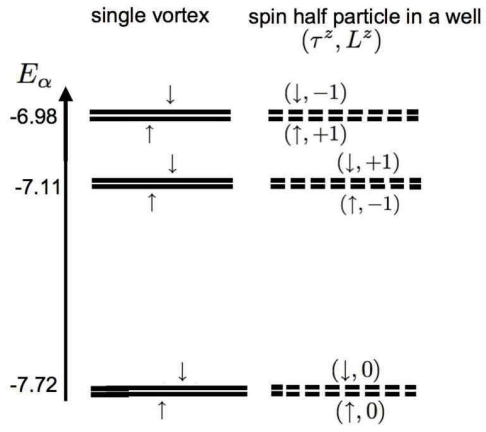


FIG. 3: Doublets of a single vortex. On the left, numerical spectrum of half filled hard core bosons on a $4\times 4$ torus, with $N_\phi = 1$, $t = 1$, and $V = 0$. Arrows denote eigenvalues of $\tau^z$. On the right, the fitted spectrum of a massive spin half particle in a continuum harmonic well with spin orbit interaction. $L^z$ labels its orbital angular momenta.

Because $\hat{\mathbf{n}}$ fluctuates, $\langle Q\rangle$ is not quantized. However, we have found that in all the single vortex eigenstates $\frac{1}{2}\text{sign}\langle Q\rangle$ correlates perfectly with eigenvalues of $\tau^z$. Moreover, in the two vortex states the total meron

| | | |
|---|---|---|
| confining force constant | $K$ | $9.9t$ |
| vortex mass | $M_{\rm v}$ | $\left(1.4-1.2\frac{V}{t}\right)\hbar^2/ta^2$ |
| spin orbit coupling | $\gamma^{\rm so}$ | $0.1a^2/\hbar$ |

TABLE I: Vortex quantum parameters. $K$ is determined variationally. The vortex mass and spin orbit coupling are extracted by fitting the spectra in Fig. (3).

charge agrees with the the $z$-component of the total v-spin.

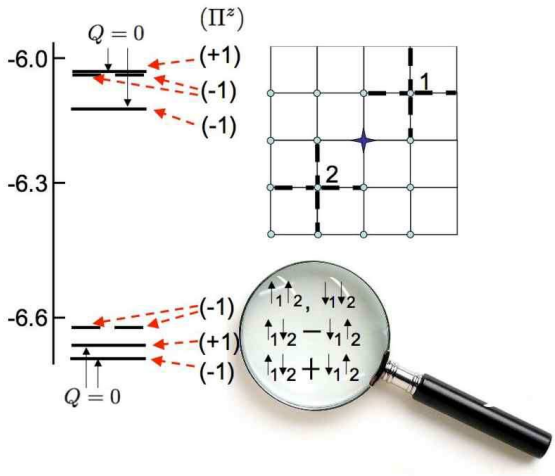


FIG. 4: Fermi-Dirac statistics of two pinned vortices. Bonds weakened by 40% (dashed lines) localize the vortices on lattice sites 1 and 2. The low energy quadruplets correspond to singlets and triplets of the two v-spins. The antiferromagnetic states exhibit $\langle Q\rangle = 0$. The orbital exchange symmetry, measured by $\Pi^z$, and the v-spin states (described in the $\tau_1^z\tau_2^z$ basis) indicate that all measured wavefunctions are antisymmetric under permutations.

**Single Vortex Hamiltonian**. For one flux quantum $N_\phi = 1$, we find that the variational energy has a quadratic minimum when the vortex center is at $\mathbf{R}_{\rm v}$ [21]. $\mathcal{H}$ is numerically diagonalized on a 4×4 lattice for $N_\phi = 1$. We fit the exact spectrum, shown in Fig. 3 to an effective hamiltonian of one spin half particle

$$\mathcal{H}_1^{\rm eff} = \frac{1}{2M_{\rm v}}\mathbf{p}^2 + \frac{1}{2}\frac{K}{L^2}\left(\mathbf{r}-\mathbf{R}_{\rm v}\right)^2 + \gamma^{\rm so}\frac{K}{L^2}\tau^z L^z. \quad (8)$$

The parameters are listed in Table I, where $L^2$ is the area of the torus. $L^z$ is the orbital angular momentum, quantized at $0, \pm 1$. The last term is a spin-orbit interaction which was introduced to lift the $L^z = \pm 1$ degeneracy, as seen in the numerical spectrum.

The most important parameter extracted from (8) is the vortex mass $M_{\rm v}$. We used two methods: (i) Using $K$ given by the variational calculation [21], and tuning $M_{\rm v}$ and $\gamma^{\rm so}$ to fit the two lowest energy spacings. (ii) Measuring the vortex zero point displacement , and fitting it to the results for Eq. (8). Here we used $|\tau^z(\mathbf{r})|$ as the vortex probability distribution in each eigenstate. The two estimates for $M_{\rm v}$ agree within our numerical uncertainty.

Defining the bosons mass to be $m_b = 0.5\frac{\hbar^2}{ta^2}$, we find that the vortex mass is not much heavier than the boson mass, and much lighter than in a weakly pinned, high density Bose condensate and a BCS superconductor [11]. Thus we see that $\mathcal{H}$ allows significant vortex delocalization, which makes the notion of vortex statistics physically relevant.

**Vortex Exchange.** We set $N_\phi = 2$, and pin the two vortices by weakening the bonds connected to sites 1 and 2 by 40% as depicted in Fig. 4. The vortices' localization is confirmed by the current density maps of the low eigenstates.

As expected for two localized spin half particles, the low energy spectrum contains quadruplets. We measure the orbital exchange symmetry using $\Pi^z$, which remains a symmetry of $\mathcal{H}$ in the presence of the pinning. The $z$-component v-spin correlations are measured by $S^{zz} = \langle\tau^z(\mathbf{r}_1)\tau^z(\mathbf{r}_2)\rangle$, and $\langle Q\rangle$.

In each quadruplet, we find two degenerate orbitally antisymmetric states $\Pi^z = -1$ which exhibit ferromagnetic correlations $S^{zz} > 0$, and sign $\langle Q\rangle = \pm 1$. The other two states exhibit $S^{zz} < 0$, $\Pi^z = \pm 1$, and $\langle Q\rangle = 0$ within numerical precision. We measure their planar correlations using

$$S^{\perp} = \langle a_1^\dagger e^{i\int_1^2 d\mathbf{l}\cdot\mathbf{A}} a_2 + \text{h.c}\rangle \quad (9)$$

The $\Pi^z = +1$ state has $S^\perp < 0$, which implies a total v-spin singlet $\tau = 0$. The $\Pi^z = -1$ state has $S^\perp > 0$, which indicates $\tau = 1$. That is to say, all states obey the relation $(-1)^\tau \Pi^z = +1$. This reflects total antisymmetry under permutation, consistent with Fermi-Dirac (and not Bose-Einstein) statistics.

**The Multi-Vortex Hamiltonian**. Next, we study the spectrum of two free vortices with no weakened bonds. Energies and wavefunctions are consistent with two spin half fermions, with mass $M_{\rm v}$, rotating about their center of mass $\mathbf{R}_{\rm v}$ [21].

We then construct a multi-vortex effective Hamiltonian

which describes a Spin Half Fermion Plasma (SHFP),

$$\begin{aligned}
\mathcal{H}^{\rm SHFP} &= \int d^2r \sum_{s=\uparrow\downarrow} \psi_s^\dagger \left( \frac{-\hbar^2\nabla^2}{2M_v} \right) \psi_s + V^{\log} + \mathcal{H}^{\rm so}, \\
V^{\log} &= \frac{\pi t}{4} \int d^2r d^2r' \ \log(|\mathbf{r}-\mathbf{r}'|) : \rho(\mathbf{r})\rho(\mathbf{r}') : \\
&\quad - \frac{n_{\rm v}\pi^2 t}{4} \int d^2r \rho(\mathbf{r}) |\mathbf{r}|^2 \\
\mathcal{H}^{\rm so} &= \frac{1}{2}\gamma^{\rm so} \int d^2r d^2r' \ \psi^\dagger (\boldsymbol{\tau}\cdot\nabla)\psi \times \frac{\mathbf{r}-\mathbf{r}'}{|\mathbf{r}-\mathbf{r}'|^2} \rho(\mathbf{r}'),
\end{aligned} \tag{10}$$

where $\psi_s^\dagger(\mathbf{r})$ is a fermion field operator with density $\rho(\mathbf{r})$. The average vortex density is $n_{\rm v}$.

At low vortex densities, $V^{\log}$ dominates over the kinetic energy, and vortices form a Vortex Lattice (VL). This is a superfluid phase with additional v-spin correlations. If they are ferromagnetic, a boson charge density with wavevector $(\pi,\pi)$ will appear at the vortex cores, as illustrated in Fig. 2. Presently however, we do not rule out more complicated v-spin orderings. Incidentally, density modulations have been observed near vortex cores of High Tc cuprate superconductors [25] and analyzed within bosonic models [26, 27].

At a finite temperature $T_m$, dislocations melt the VL [28, 29]. The classical melting temperature is independent of vortex density (magnetic field). For the SHFP, the kinetic energy suppresses $T_m$ as a function of vortex density, until quantum melting is reached.

**The Vortex Metal**. At a critical vortex density $n_{\rm v}^{\rm cr}$ the VL melts by quantum fluctuations. We estimate $n_{\rm v}^{\rm cr}$ by mapping the fluctuations of the VL to the Wigner crystal of a two dimensional electron gas [30], which melts at $n_e^{\rm cr}$. (Henceforth we neglect $\mathcal{H}^{\rm so}$). A simple relation is obtained:

$$n_{\rm v}^{\rm cr} = 0.026 \frac{M_v t}{\hbar^2} \sqrt{n_e^{\rm cr}} a_B, \tag{11}$$

where $a_B$ is the Bohr radius. Tantar and Ceperley [31] have evaluated $n_e^{\rm cr} = 1/(37 a_B)^2$, by variational Monte Carlo methods. Taking their result at face value, and using the vortex mass from Table I, the critical melting density of the SHFP is estimated at

$$n_{\rm v}^{\rm cr} a^2 = (9.8 - 8.4\, V/t) \times 10^{-4}. \tag{12}$$

For $n_{\rm v} > n_{\rm v}^{\rm cr}$, the SHFP turns into a Vortex Metal (VM), a two dimensional Fermi liquid.

The VM may be a v-spin paramagnet or ferromagnet. The latter exhibits a charge density wave. The characteristic Fermi temperature is

$$T_F = \nu \frac{\pi \hbar^2 n_{\rm v}}{M_{\rm v}} \tag{13}$$

where $\nu = 1(2)$ for the v-spin paramagnet (ferromagnet). The Fermi temperature determines both thermodynamic and transport properties of the VM. For example, the specific heat should be linear in $T/T_F$.

The vortex conductivity is expected to saturate at low temperatures due to residual scattering of impurities. In normal metals the resistivity increases with temperature, due to inelastic scattering. By vortex-charge duality, the resistivity equals vortex conductivity [32]. We therefore expect the resistivity in the VM phase, to initially *decrease* with rising temperature. This would be an unusual behavior resembling a Kondo effect.

**Discussion**. For $N_\phi = 1$, we have proven doublet degeneracies for a vortex centered on any lattice site. The doublet degeneracies are slightly lifted as the AB fluxes move the $\mathbf{R}_{\rm v}$ between lattice sites, although no level crossings between lowest doublets were observed.

At half filling the particle-hole symmetry *exposed* the v-spin via Kramers degeneracies. Away from half filling, a 'Zeeman field' will polarize the v-spin into the $xy$ plane, and a Magnus term will enter the vortex hopping. We nevertheless find the v-spin and Fermi statistics to be relatively *short range* properties, which emerge on small lattices. Thus we expect the VM phase to survive small perturbations and be relevant in a region around half filling.

Direct realizations of $\mathcal{H}$ are rotating cold atoms on partially filled optical lattices [3, 4, 5], and gated low capacitance Josephson Junction arrays [20]. Quantum Hall phases of bosons, which may exhibit fermionic features, are expected at very strong rotations, (i.e. low boson filling factors) $n_{\rm v} a^2 \approx 0.5$ [33]. Our estimate in Eq. (12) expects the VM to appear at much lower vortex densities.

A less justifiable realization, but interesting nonetheless, are disordered superconductor films in a transverse field [15, 16, 17] and high $T_c$ cuprate films. These systems exhibit low superfluid density due to strong disorder, interactions and lattice effects. Although their effective boson density is not well controlled, it is conceivable that the VM may be a good starting point to describe some of their transport properties, as proposed earlier [13, 14].

Previously, Balents *et. al.* [27] have studied vortex condensates at fractional fillings $p/q$ and derived $q$-fold degenerate vortex fields. Our analysis, which treats a finite number of vortices on finite tori, agrees with their degeneracy at half filling.

Last, we comment that at finite temperatures, transport (even without external rotation or magnetic field) is dominated by motion of vortices and antivortices[8]. Finite temperature scattering rates should reflect the fact that mobile vortices (antivortices) are fermionic particles (holes), which may differ from classically diffusing charges [34]. In other words, a modified theory of finite temperature transport for hard core bosons is called for.

**Acknowledgements.** We thank Ehud Altman, Yosi Avron, Herb Fertig, Gil Refael and Efrat Shimshoni for useful discussions. Support of the US Israel Binational

Science Foundation is gratefully acknowledged. AA acknowledges the Aspen Center For Physics where some of the ideas was conceived.


[1] L. N. Cooper, Phys. Rev. **104**, 1189 (1956).
[2] F. Wilczek, Phys. Rev. Lett. **49**, 957 (1982).
[3] M. R. Matthews, B. P. Anderson, P.C. Haljan, D. S. Hall, C. E. Wieman, E. A. Cornell, *Phys. Rev. Lett.* **83**, 2498, (1999).
[4] K.W. Madison, F. Chevy, W. Wohlleben,J. Dalibard, *Phys. Rev. Lett.* **84**, 806 (2000).
[5] J. R. Abo-Shaeer, *et. al.* , Science, **292**, 476 (2001).
[6] J.M. Kosterlitz and D.J. Thouless, Jour. Phys. C **6**, 1181 (1973).
[7] M. Tinkham, *Introduction to Superconductivity*, (Krieger, NY (1980)).
[8] V. Ambegaokar, B. I. Halperin, and D. R. Nelson, and E.D. Siggia, *Phys. Rev. B* **21**, 1806 (1980).
[9] Q. Niu, P. Ao and D. J. Thouless, Phys. Rev. Lett., **72**, 1706 (1994).
[10] D. P. Arovas and J. A. Freire, *Phys. Rev. B* **55**, 1068 (1997).
[11] A. Auerbach, D. P. Arovas and S. Ghosh, Phys. Rev. B74, 64511, (2006).
[12] M. P. A. Fisher and D. H. Lee, Phys. Rev. B **39**, 2756 (1989).
[13] P. Phillips and D. Dalidovich, Science, **302**, 5643 (2003);
[14] V. M. Galitski, G. Refael, M. P. A. Fisher, T. Senthil, Phys. Rev. Lett. **95**, 077002 (2005).
[15] D. Ephron, A. Yazdani, A. Kapitulnik, and M. R. Beasley, Phys. Rev. Lett. 76, 1529 (1996).
[16] N. Mason and A. Kapitulnik, Phys. Rev. B **64**, 60504 (2001).
[17] G. Sambandamurthy, L. W. Engel, A. Johansson, D. Shahar, Phys. Rev. Lett. **92**, 107005 (2004);
[18] D. Arovas, J. R. Schrieffer, and F. Wilczek, Phys. Rev. Lett. **53**, 722 (1984).
[19] The Berry phase procedure fails due to the slow decay of the vortex core density depletion at large distances, as shown by F. D. M. Haldane and Y.-S. Wu, Phys. Rev. Lett. **55**, 2887 (1985).
[20] A. van Oudenaarden and J. E. Mooij, Phys. Rev. Lett. **76**, 4947 (1996).
[21] See Supplemental Material.
[22] $\mathcal{H}$ is precisely represented by the gauged quantum XXZ model [21]).
[23] R. Tao and F. D. M. Haldane, Phys. Rev. B **33**, 3844 (1986).
[24] E. Altman and A. Auerbach, Phys. Rev. Lett. **81**, 4484 (1998).
[25] J. E. Hoffman, E. W. Hudson, K. M. Lang, V. Madhavan, H. Eisaki, S. Uchida, J. C. Davis, Science **295**, 466 (2002).
[26] H.-D. Chen, O. Vafek, A. Yazdani and S.-C. Zhang, Phys. Rev. Lett. **93**, 187002 (2004)
[27] L. Balents, L. Bartosch, A. Burkov, S. Sachdev, and K. Sengupta, Phys. Rev. B **71**, 144508 (2005).
[28] S. Doniach and B.A. Huberman, PRL 17, 1169 (79).
[29] D. S. Fisher, Phys. Rev. B **22**, 1190 - 1199 (1980).
[30] We thank Herb Fertig for pointing out that quantum melting is determined primarily by short range interactions.
[31] B. Tanatar and D. M. Ceperley, Phys. Rev. B **39**, 5005,(1989).
[32] D. Shahar, D. C. Tsui, M. Shayegan, E. Shimshoni, and S. L. Sondhi, Science **274**, 589 (1996).
[33] J.W. Reijnders, F.J.M van Lankvelt, K. Schoutens, N. Read, Phys. Rev. A **69**, 023612 (2004).
[34] N. Lindner and A. Auerbach, unpublished.

## I. SUPPLEMENTAL MATERIAL

### A. The Hamiltonian in the Spin Representation

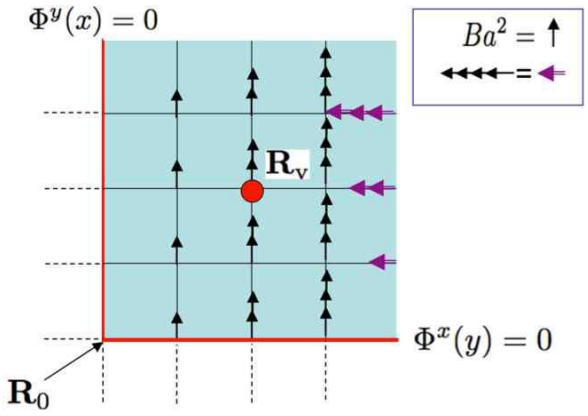


FIG. 5: The gauge field choice of the hard core boson model. The direction of $\mathbf{A}$ is marked by arrows, whose magnitudes are explained in the legend. A null point $\mathbf{R}_0$ is the intersection of two zero flux orbits marked by red lines. $\Phi^\alpha(x_\beta)=\oint dx^\alpha A_\alpha$ are Wilson loop functions. The vortex center of mass $\mathbf{R}_\mathrm{v}$ is marked by the red circle. In this figure, the Aharonov Bohm fluxes are set to zero $\mathbf{\Theta}=0$, and the null point is precisely on the left bottom lattice site.

The lattice bosons hamiltonian (1), is faithfully represented by the gauged Quantum XXZ Model

$$\mathcal{H}=\sum_{\langle \mathbf{r},\mathbf{r}'\rangle}\frac{-t}{2}\left(e^{i\int_{\mathbf{r}}^{\mathbf{r}'}d\mathbf{l}\cdot\mathbf{A}}S^+_{\mathbf{r}}S^-_{\mathbf{r}'}+\mathrm{h.c.}\right)+VS^z_{\mathbf{r}}S^z_{\mathbf{r}'} \quad (14)$$

where the sum is over bonds of the square lattice, and the hard core boson operators in (1) are represented by spin half operators

$$a_{\mathbf{r}}=S^-_{\mathbf{r}},\qquad a^\dagger=S^+_{\mathbf{r}},\qquad n_{\mathbf{r}}=S^z_{\mathbf{r}}+\frac{1}{2}. \quad (15)$$

The number of lattice sites in the both directions is $\mathbf{N}=\mathbf{L}/a$, and the lattice positions are labelled by $n_\alpha=0,1,\dots N_\alpha-1$, $\alpha=x,y$. The $\mathbf{\Theta}=0$ gauge field is chosen as shown in Fig. 5:

$$\begin{aligned}A^x_{\mathbf{r},\mathbf{r}+a\hat{\mathbf{x}}} &= -yBL_x\delta_{n_x,N_x-1}+\Theta_x/N_x\\ A^y_{\mathbf{r},\mathbf{r}+a\hat{\mathbf{y}}} &= xBa+\Theta_y/N_x\end{aligned} \quad (16)$$

where $B=\frac{2\pi N_\phi}{L_xL_y}$, where the flux quantum is $2\pi$. The gauge invariant content of $\mathbf{A}$ are the uniform magnetic field with flux $Ba^2$ in each plaquette, and two Wilson loop functions defined as $\Phi^x(y)=\oint dxA^x(x,y)$, and similarly for $\Phi^y(x)$. Explicitly,

$$\begin{aligned}\Phi^y(x) &= xBL_y+\Theta^y\\ \Phi^x(y) &= -yBL_x+\Theta^x\end{aligned} \quad (17)$$

A special gauge invariant point on the torus is a null point $\mathbf{R}_0$ given by the condition $\Phi^y=\Phi^x=0$. $\mathbf{R}_0$ is the intersection of the two zero flux orbits depicted by red lines in Figs. 1,5. For $\mathbf{\Theta}=0$ we calibrate $\mathbf{R}_0=(0,0)$. Changing the AB fluxes $\mathbf{\Theta}$ yields

$$\mathbf{R}_0(\mathbf{\Theta})=\frac{1}{2\pi N_\phi}\mathbf{L}\times\mathbf{\Theta}\ \mod\mathbf{L} \quad (18)$$

The antipodal point is $\mathbf{R}_\mathrm{v}(\mathbf{\Theta})=\mathbf{R}_0+\frac{1}{2}\mathbf{L}$. $\mathbf{R}_\mathrm{v}$ turns out to be a point of minimal variational energy for the vortex center of mass.

### B. Symmetry Operators

Let us set $\mathbf{\Theta}$, such that $\mathbf{R}_\mathrm{v}(\mathbf{\Theta})$ is a lattice symmetry point. These include, in particular, any lattice site, center of a bond, or center of plaquette. The reflection operators at position $\mathbf{R}_\mathrm{v}=(X_\mathrm{v},Y_\mathrm{v})$ are defined by

$$\begin{aligned}P^x[\mathbf{R}_\mathrm{v}]:&\quad x-X_\mathrm{v}\to X_\mathrm{v}-x,\quad A^x\to -A^x,\\ P^y[\mathbf{R}_\mathrm{v}]:&\quad y-Y_\mathrm{v}\to Y_\mathrm{v}-y,\quad A^y\to -A^y,\end{aligned} \quad (19)$$

where we omit the variables which do not change under the transformations. It is easy to verify that $P^\alpha$ sends $B\to -B$ and inverts both Wilson loop functions $\Phi^\alpha\to -\Phi^\alpha \mod 2\pi$. The charge conjugation operator acts on the boson variables as

$$\begin{aligned}&C\equiv e^{i\pi\sum_{\mathbf{r}}S^x_{\mathbf{r}}}\\ &\mathcal{H}[\mathbf{A}]\to\mathcal{H}[-\mathbf{A}]\end{aligned} \quad (20)$$

Now, we construct two symmetry operators

$$\Pi^\alpha[\mathbf{R}_\mathrm{v}]=U^\alpha CP^\alpha[\mathbf{R}_\mathrm{v}],\qquad \alpha=x,y \quad (21)$$

Where $U^\alpha[\mathbf{A},\mathbf{R}_\mathrm{v}]$ is a gauge transformation, explicitly given for the gauge choice in Eq. (16) as

$$\begin{aligned}U^\alpha &= e^{i\sum_{\mathbf{r}}\chi^\alpha(\mathbf{r};\mathbf{R}_\mathrm{v})S^z_{\mathbf{r}}}\\ \chi^x(\mathbf{r};\mathbf{R}_\mathrm{v}) &= y\left(\theta_{2D-x}-\theta_{x-2X_v}-1\right)BL_x\\ \chi^y(\mathbf{r};\mathbf{R}_\mathrm{v}) &= -2x(Y_\mathrm{v}-L_y/2)B\end{aligned} \quad (22)$$

where $D=X_\mathrm{v}-L_x/2$ and $\theta_x$ is the Heavyside function. $U^\alpha$ restores the gauge field in $\mathcal{H}[\mathbf{A}]$ after the action of $CP^\alpha$. It is now possible to verify that $\Pi^\alpha$ are symmetries of $\mathcal{H}$:

$$\left[\mathcal{H}[\mathbf{\Theta}],\Pi^\alpha[\mathbf{R}_\mathrm{v}(\mathbf{\Theta})]\right]=0,\quad \alpha=x,y. \quad (23)$$

It is possible to construct $U^\alpha$, only because $CP^\alpha$ leave $B$, $\Phi^x$ and $\Phi^y$ invariant, since we have chosen the reflections about the symmetry point $\mathbf{R}_\mathrm{v}$.

A straightforward but rather lengthy calculation, yields the commutation relation between the two operators:

$$\Pi^y(\mathbf{R}_\mathrm{v})\Pi^x(\mathbf{R}_\mathrm{v}) = (-1)^{N_\phi(2X_v/a+1)(2Y_v/a+1)} \times \Pi^x(\mathbf{R}_\mathrm{v})\Pi^y(\mathbf{R}_\mathrm{v}) \quad (24)$$

Note that adding to $\chi^\alpha$ in (22) any constant, multiplies the left hand side of (24) by a gauge transformation $e^{i\zeta S^z_{\rm tot}}$. At half filling of an even number of lattice sites, $S^z_{\rm tot}=0$.

Therefore $\Pi^x(\mathbf{R}), \Pi^y(\mathbf{R})$ will *anticommute* for any odd number of fluxes $N_\phi$, as long as $\mathbf{R}_\mathrm{v}$ is *on a lattice site*. We now add another operator $\Pi^z = -i\Pi^x\Pi^y$, and verify that for $\alpha = x, y, z$,

$$\Pi^\alpha = (\Pi^\alpha)^\dagger = (\Pi^\alpha)^{-1} \qquad \Rightarrow (\Pi^\alpha)^2 = 1. \quad (25)$$

An SU(2) spin half algebra of v-spin operators, is thus constructed

$$[\tau^\alpha, \tau^\beta] = i\epsilon_{\alpha\beta\gamma}\tau^\gamma \quad (26)$$

where $\epsilon$ is the antisymmetric tensor. $\boldsymbol{\tau}$ describes the v-spin of a single vortex $N_\phi = 1$ centered at $\mathbf{R}_\mathrm{v}$. $\Pi^z$ describes a global rotation by 180° about $\mathbf{R}_\mathrm{v}$, which will be useful for the two vortex symmetry analysis.

### C. Variational Vortex Potentials

The variational energy of $\mathcal{H}$, on a square lattice of length $L$, is simply the classical energy

$$\langle\{\theta\}|\mathcal{H}|\{\theta\}\rangle = -t\sum_{\langle \mathbf{r},\mathbf{r}'\rangle}\cos\left(\theta_\mathbf{r} - \theta_{\mathbf{r}'} - \int_\mathbf{r}^{\mathbf{r}'} d\mathbf{l}\cdot A\right) \quad (27)$$

where we use spin coherent states, with all spins parametrized by angles $\theta_\mathbf{r}$ in the $xy$ plane. Using dimensionless complex coordinates $\mathbf{r} \to z = (x+iy)/L$, and $\mathbf{R}_\mathrm{v} \to Z_\mathrm{v} = (X_\mathrm{v} + iY_\mathrm{v})/L$, a vortex on a torus centered at $Z_\mathrm{v}$ is described by a Jacobi theta function:

$$\theta(z, Z_\mathrm{v}) = -\mathrm{Im}\log\vartheta\big(i(z-Z_\mathrm{v}) - 1/2 - i/2\big) + \pi\,(y - (1/2 - Y_\mathrm{v})x)$$
$$\vartheta(z) = \sum_{n=-\infty}^{\infty} e^{-\pi n^2} e^{2i\pi n z}. \quad (28)$$

For multiple vortices, we take a superposition of single vortex configurations

$$\theta^N(z; z_v^1, ..., z_v^{N_\phi}) = \sum_{i=1}^{N_\phi}\theta(z; z_v^i). \quad (29)$$

The resulting potential energy for the vortices is

$$U\big(\mathbf{r}_1, \mathbf{r}_2, \ldots, \mathbf{r}_N; \mathbf{R}_\mathrm{v}\big) = \langle\theta^N|\mathcal{H}|\theta^N\rangle \quad (30)$$

For a single vortex on a square lattice of length $L$ we find that

$$U = \frac{1}{2}K|\mathbf{r}_1 - \mathbf{R}_\mathrm{v}|^2/L^2, \qquad K = 9.9t. \quad (31)$$

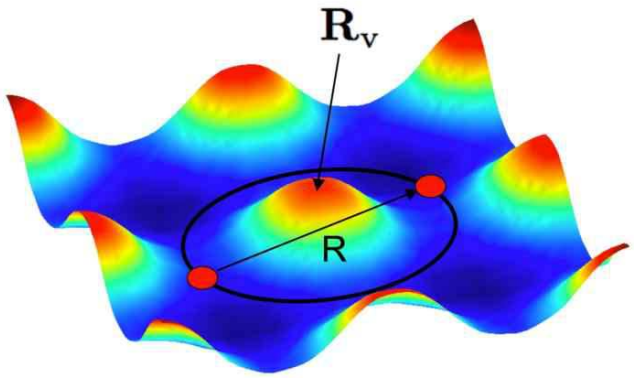


FIG. 6: The potential energy for two vortices. The variational energy of Eq. (27) is plotted as a function of one vortex position $\mathbf{r}_1 = -\mathbf{r}_2$. The center of mass is fixed at $\mathbf{R}_\mathrm{v}$. The vortices (marked by red filled circles) rotate around $\mathbf{R}_\mathrm{v}$ on the circle of diameter $R$. This potential justifies the effective rotator model (32) used to fit the spectrum in Fig. 7.

### D. Two Unpinned Vortex Spectrum

When we restore the weakened bonds of Fig. 4 to the uniform value $-t$, the two vortices spectrum at $N_\phi = 2$ ceases to exhibit well separated low lying quadruplets.

For two vortices, we place the center of mass at $\mathbf{R}_v$, (which by the way is equivalent to $\mathbf{R}_0$ because of the torus periodicity). $U$ of (30) is minimized at four values of the $\mathbf{r}_1, \mathbf{r}_2$, which keep them furthest away from $\mathbf{R}_0, \mathbf{R}_\mathrm{v}$ and from each other. This is illustrated in Figure 6. Thus, the low energy effective Hamiltonian of two vortices describes collective rotation around $\mathbf{R}_\mathrm{v}$.

We fit the spectrum, shown in Fig. 7, with a Hamiltonian for the relative motion of two spin half fermions

$$\mathcal{H}_2^{\rm eff} = \frac{(L^z_{\rm rel})^2}{M_v R^2} + \gamma_2^{\rm so} L^z_{\rm rel}\tau^z_{\rm tot}. \quad (32)$$

$M_\mathrm{v}$ is taken from Table I and the vortex separation on the 16 site lattice is, $R \approx 2\sqrt{2}a$. The relative angular momentum of the vortices is $L^z_{\rm rel}$, which is quantized in integer units. $\gamma_2^{\rm so}$ is spin orbit parameter chosen at $\sim 0.15t$, for a best fit to the numerical spectrum in Fig. 7. It roughly agrees with the assignment of $\gamma^{\rm so}$ in Table I. As shown in the Fig 4, the wavefunctions symmetries and v-spin correlations are fully consistent two spin half interacting fermions.

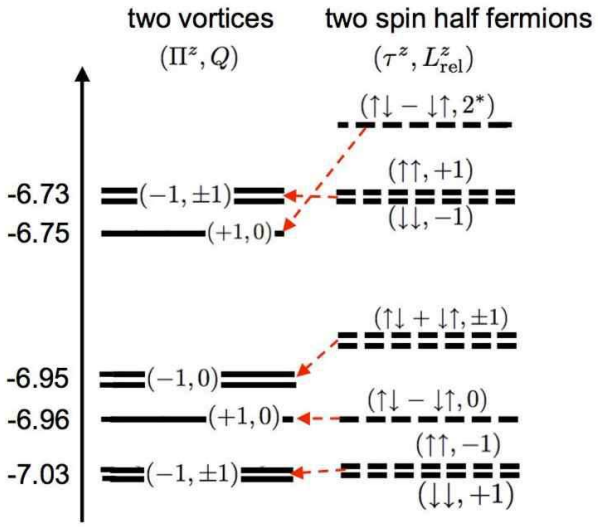


FIG. 7: Two unpinned vortices. On the left: the lowest spectrum of Eq. (1) with $N_\phi = 2$. Eigenvalues of orbital exchange symmetry $\Pi^z$, and assigned meron charges $Q$ are listed. On the right: spectrum of Eq. (32), describing a rotator with total v-spin $\tau^z$, and oribital angular momentum $L^z_{\rm rel}$, in a potential described by Fig. 6. The angular momentum marked by $*$ is non degenerate due to the lattice symmetry.